DACOMAT

**Deliverable number: D1.4**


# Fatigue model based on a cohesive law

**Stergios Goutianos**

**DTU**

The DACOMAT project has received funding from the European Union's Horizon 2020 research and innovation programme under GA No. 761072

# Deliverable details

Document name: D1.4 Fatigue model based on a cohesive law

Responsible partner: Technical University of Denmark (DTU)

Work package: WP1

Task: 1.4

Due date: 31.12.2019

Delivery date: 23.12.2019

| Dissemination level | |
|---|---|
| x | PU = Public |
| | CO = Confidential, only for members of the consortium (including the EC) |
| | Classified, information as referred to in Commission Decision 2001/844/EC. |
| **Deliverable type** | |
| x | R: Document, report (excluding the periodic and final reports) |
| | DEM: Demonstrator, pilot, prototype, plan designs |
| | DEC: Websites, patents filing, press & media actions, videos, etc. |
| | OTHER: Software, technical diagram, etc. |



The DACOMAT project has received funding from the European Union's Horizon 2020 research and innovation programme under GA No. 761072

# Popular science summary

A wind turbine blade in operation is subjected to cyclic loads. Similarly, a bridge is also subjected to cyclic loading due to passing traffic. A material can be weakened by cyclic loading even if the maximum cyclic load is lower than the minimum load that can fully break the material. The material weakening under cyclic loading is called fatigue and results in progressive damage and growth of microcracks. Microcracks can propagate and merge to larger cracks, which once they reach a critical size can cause material failure (complete fracture of a structure). In DACOMAT, we aim to develop numerical models that will enable fatigue modelling of various composite structures. We aim to develop two methods. The first method models progressive fatigue crack growth for many cycles. Typically, a structure will fail by fatigue damage after some millions of cycles. Consequently, this modelling approach can result in time-consuming calculations. The second approach we aim to develop transforms the cyclic problem to a static problem that can be solved with one simulation run and therefore are a lot more computationally efficient. The two approaches are described in this report.

The DACOMAT project has received funding from the European Union's Horizon 2020 research and innovation programme under GA No. 761072

**Contents**



The DACOMAT project has received funding from the European Union's Horizon 2020 research and innovation programme under GA No. 761072

## 1. Summary

The aim of the work presented in this report is to develop a computational model suitable for simulating fatigue driven crack growth with reasonable computational cost. To accomplish this task, two approaches have been evaluated:

Approach A: Formulate, implement and validate a cyclic cohesive element, that can be used in a commercial finite element software.

Approach B: Develop a new tool where the fatigue crack extension problem is transformed through mathematical scaling to an equivalent static problem. This approach is significantly less computationally demanding and easier to solve.

Both approaches present significant challenges, however approach A is somewhat more conventional. It was, thus, stated that approach A would be given priority, as the risk of implementing approach B is higher.

In the first part of present report, the implemented cyclic cohesive element is briefly described. Simple examples used as validation are given, followed by a list of future developments, within the project, to make the element more versatile.

In the second part of the report, the work performed for approach B is presented. The different cyclic cohesive laws developed are presented. These cohesive laws are used in a simple model to test the scaling method. All the tools needed for approach B are developed and in the next project period, the scaling approach will be examined more thoroughly.

The DACOMAT project has received funding from the European Union's Horizon 2020 research and innovation programme under GA No. 761072

## 2. Approach A: Cyclic cohesive element

In this Section, the implementation of the cyclic cohesive element to simulate fatigue driven crack growth is presented. The cyclic cohesive element is programmed in a user defined element subroutine for the Abaqus commercial finite element software.

### 2.1 Background

Cohesive element formulations to simulate initiation and propagation of cracks in composites under cyclic loading have been the subject of research over the last decades (Davila, 2018). Several cyclic cohesive elements have been proposed for modelling cyclic crack growth, for example by Roe & Siegmund, 2003 and Nguyen, Repetto, Ortiz, & Radovitzky, 2001. For a more detailed list of various cyclic cohesive elements, the reader is referred to the review paper of Bak, Sarrado, Turon, & Costa, 2014. The main challenge in formulating a cyclic cohesive element is to relate the fatigue damage to the crack propagation rate (Bak, Turon, Lindgaard, & Lund, 2017, Davila, 2018).

Among the various proposed cyclic cohesive element formulations, it was decided to focus on the formulation recently developed by Davila, 2018. The advantages of this formulation will be described in the next Section 2.2.

### 2.2 Cyclic cohesive damage model

Consider a two-dimensional solid subjected to a cyclic load. A fatigue crack is assumed to initiate and grow at the centre of the specimen as shown in Figure 1. The fatigue crack is modelled (in a finite element model) with a cohesive element whose response can describe fatigue damage accumulation. The cyclic load in the fatigue crack (or cohesive element) is shown in Figure 1. In the following, it is assumed that the fatigue crack initiates and grows under pure mode I (normal crack opening).

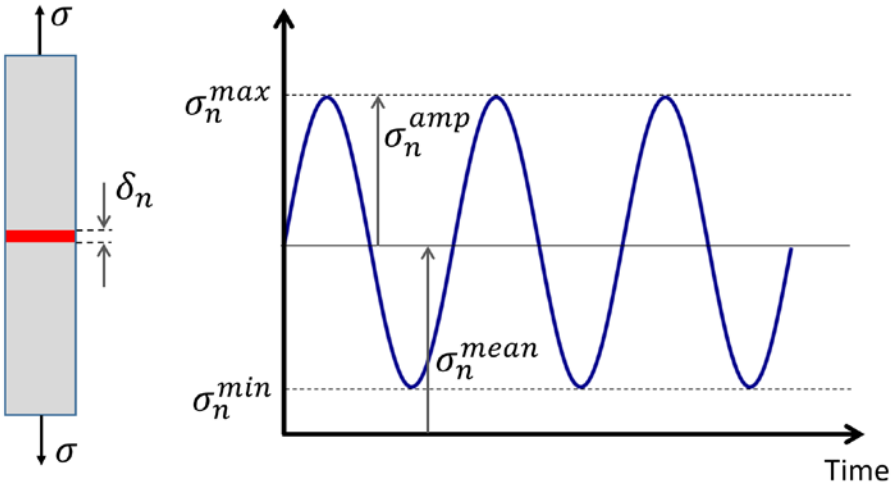


**Figure 1** Cyclic loading.

Figure 2 shows the shape of cohesive law. The initial rising part, up to $\hat{\sigma}_n$ (normal peak traction), represents the elastic response under static loading. The linear softening from $\hat{\sigma}_n$ to zero traction corresponds to damage under static loading. These two curves define the envelope of the damage process (Davila, 2018) e.g. any point outside corresponds to failure state.

If the cyclic loading, $\sigma_n^{max}$, is less that the peak traction, $\hat{\sigma}_n$, then fatigue damage accumulation occurs. The maximum normal opening, $\delta_n$, increases from point A to point B (see Figure 2). At point B, the

The DACOMAT project has received funding from the European Union's Horizon 2020 research and innovation programme under GA No. 761072

boundaries of the damage envelope are reached leading to unstable failure. This is one the advantages of the model by Davila, 2018 e.g. it includes both static and fatigue damage.

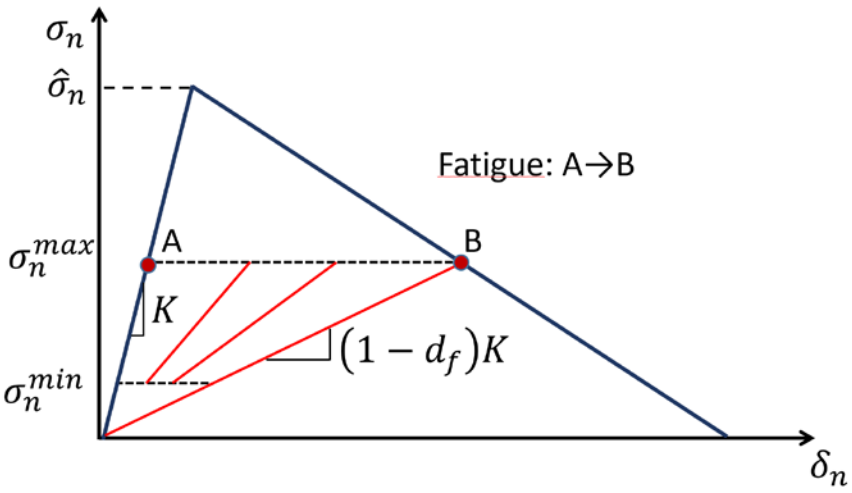


**Figure 2** Fatigue under constant stress ($\sigma_n^{max}$).

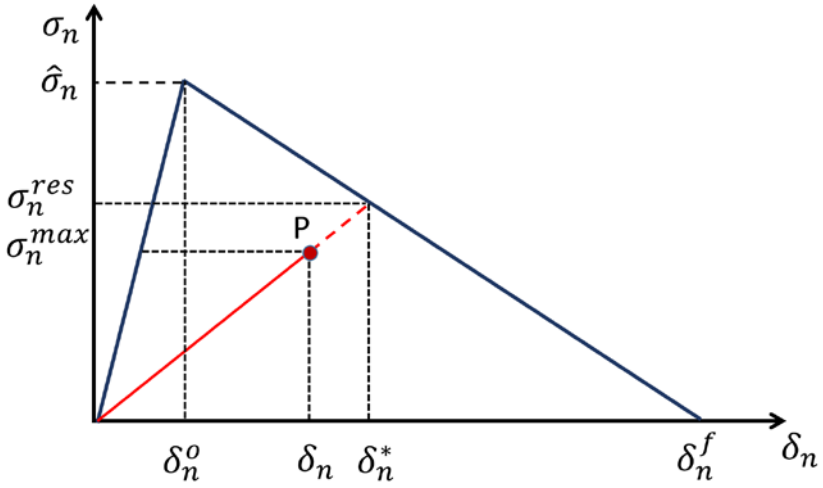


**Figure 3** Definition of openings and tractions in fatigue.

The fatigue damage accumulation model (Davila, 2018) is given by:

$$\frac{dD}{dN} = (D + \gamma_f)\left(\frac{\delta_n}{\delta_n^*}\right)^{\beta_f} \quad 1$$

where the damage norm $D$ is:

$$D = \frac{\delta_n^* - \delta_n^o}{\delta_n^f - \delta_n^o} \quad 2$$

The DACOMAT project has received funding from the European Union's Horizon 2020 research and innovation programme under GA No. 761072

where the openings are defined in Figure 3. The normal opening at any point between A and B (see Figure 2) is:

$$\frac{\delta_n}{\delta_n^*} = \frac{\sigma_n^{max}}{(1-D)\hat{\sigma}_n} \qquad 3$$

From the damage norm, $D$, the fatigue loss of stiffness (see Figure 2) can be calculated:

$$\left(1 - d_f\right) = \frac{\delta_n^* - \delta_n^f \, D}{\delta_n^*} \qquad 4$$

As can be seen from Eq. 1, the fatigue damage accumulation depends on two parameters ($\beta_f$ and $\gamma_f$). A key feature of this model is that the damage is local e.g. the fatigue damage accumulation at a material point does not depend on the damage state at other locations as it is assumed in many cyclic cohesive laws. Eq. 1 is selected in such way as to predict the propagation rate of crack according to Paris law (Paris, Gomez, & Anderson, 1961). It should be emphasized, however, that Eq. 1 predicts the propagation rate and does not impose a fatigue crack growth rate according to Paris law.
An additional advantage of the model of Davila, 2018 is that fatigue damage can occur without the need to first reach the normal peak traction, $\hat{\sigma}_n$.

## 2.3 Implementation details

The fatigue damage model of the previous Section was implemented in the Abaqus finite element software as a cohesive constitutive model. A user-defined material subroutine (UMAT) was developed.

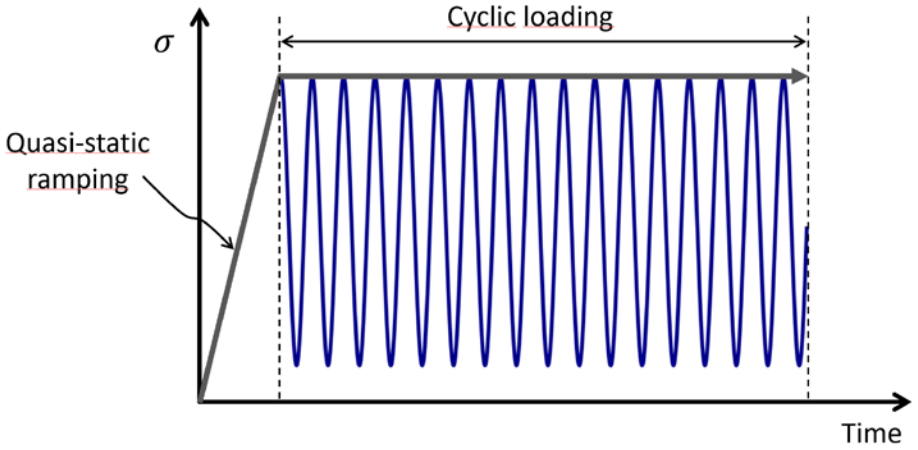


**Figure 4** The simplified cyclic loading procedure *(Bak, Turon, Lindgaard, & Lund, 2017)*.

In order to improve computational efficiency, the approach adopted was to use the simplified cyclic loading procedure (Bak, Turon, Lindgaard, & Lund, 2017) shown in Figure 4. Since it is computational expensive to cycle the applied load, in the simplified cyclic loading procedure the load (or stress in the simple example of Figure 2) is held constant. If it is assumed that the frequency of the cyclic loading is 1Hz, then the analysis time (Figure 4) corresponds to the number of cycles. The effect of cycling on fatigue damage is included in the constitutive law. Effects such as the R-ratio are also included in the fatigue damage model by modifying accordingly the parameters $\beta_f$ and $\gamma_f$.

The DACOMAT project has received funding from the European Union's Horizon 2020 research and innovation programme under GA No. 761072

Figure 5 shows the part of an Abaqus input file where the parameters of the cohesive element constitutive model is entered. The first six entries define the mode I and mode II static cohesive laws (or the damage envelope), whereas the last two parameters are related to the damage model.

```
*Material, name=CyclicCohesive
*user material, constants=8
**Kn      Kt      Smax    Tmax    G1      G2      Beta_f  Gamma_f
10.0,     10.0,   1.0,    1.0,    0.5,    0.5,    15.0,   0.9535
```

**Figure 5** Example of an Abaqus input file defining the fatigue damage model thought the last two variable: *Beta_f* $\rightarrow\beta_f$ and *Gamma_f* $\rightarrow\gamma_f$.

## 2.4 Simple examples

Figure 6 shows the cyclic normal opening of a cohesive element representing the model shown in Figure 2. In this case, a single cohesive element was used for the cohesive zone (red area in Figure 2). The two loading steps, a quasi-static and cyclic loading can be seen. It should be mentioned that the analysis is not performed for every cycle. It is possible to set a maximum number of cycles per increment. This increases the computationally efficiency significantly. However, it is recommended not to set a very high maximum number of cycles per increment.

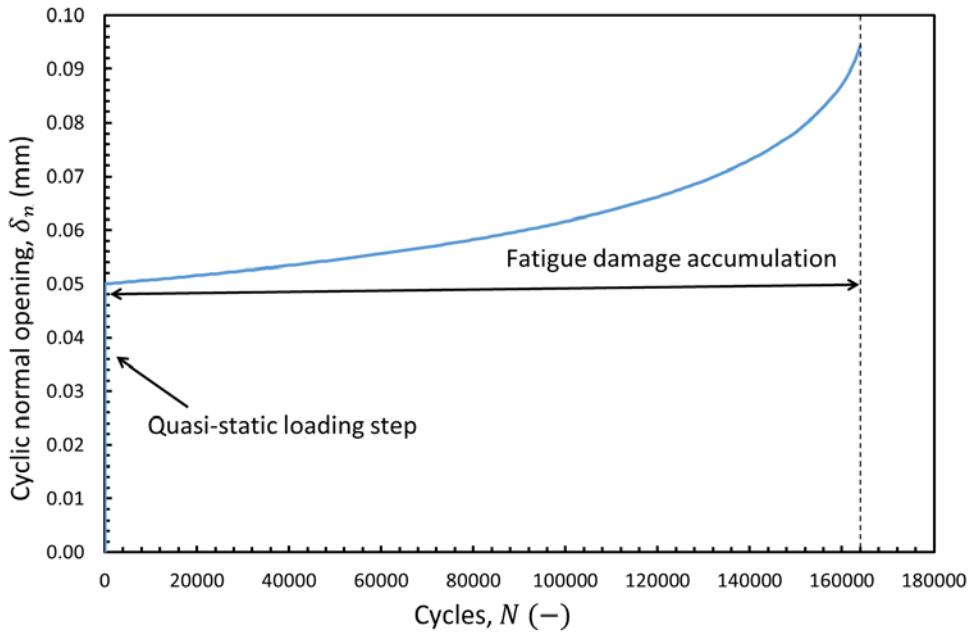


**Figure 6** Example: Normal opening of a cohesive element (see Figure 2) under cyclic loading. $\beta_f = 18.0$ and $\gamma_f = 0.0372684$.

Figure 7 shows a second example of the model of Figure 2. In this case, the input file (see Figure 5) is modified to include two pairs of $\beta_f$ and $\gamma_f$ with each pair corresponding to a different R-ratio.

The DACOMAT project has received funding from the European Union's Horizon 2020 research and innovation programme under GA No. 761072

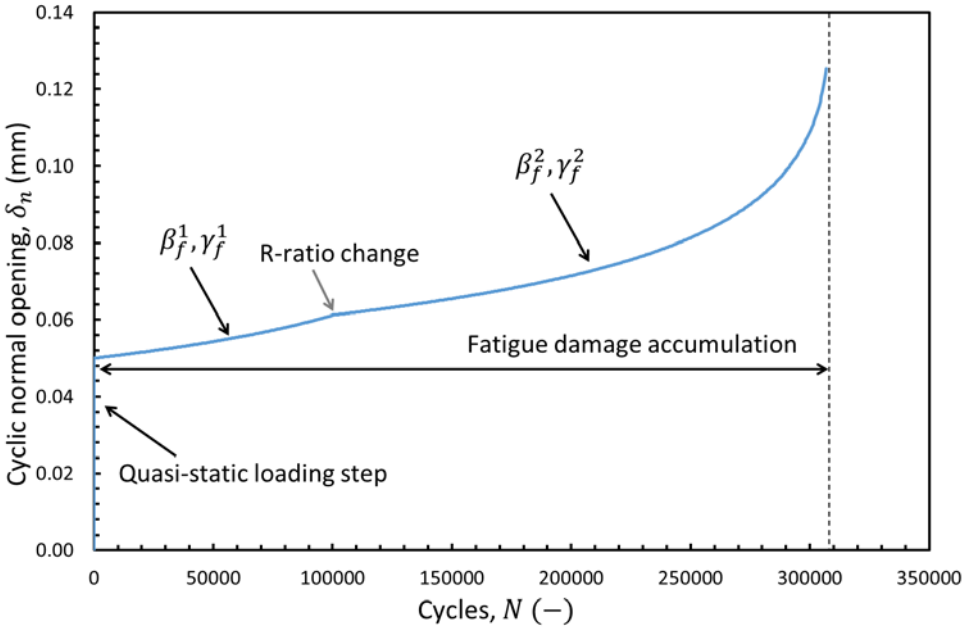


**Figure 7** Example: Normal opening of a cohesive element (see Figure 2) under cyclic loading with an R-ratio change at $N = 100000$ ($[\beta_f^1, \gamma_f^1] \rightarrow [\beta_f^2, \gamma_f^2]$).

## 2.5 Future developments

The basic implementation of the cyclic cohesive law has been implemented and validated through simple examples. There are several improvements that can be made in order to make the model more general.

a) Add the mode II component, and thus include also mix-mode fatigue crack growth.
b) The current model can predict crack growth according to Paris law. Superimposing, a cohesive element with bi-linear softening law (see D1.3), will allow to capture the R-effect (Davila, 2018).
c) The parameters for the fatigue damage accumulation model will be experimentally measured in WP3 where cyclic DCB tests will be performed.

The DACOMAT project has received funding from the European Union's Horizon 2020 research and innovation programme under GA No. 761072

# 3. Approach B: Scaling cyclic loading to an equivalent static problem

The Approach A (Section 2) is the traditional approach for fatigue analysis. The model selected (Davila, 2018) has several advantages over most existing models. However, it is still computationally expensive and probably unattractive for design (industrial) purposes. For this reason, an alternative method is also developed in parallel with Approach A. In this method (Approach B), the fatigue crack extension problem is transformed through mathematical scaling to an equivalent static problem, which is significantly easier to solve.

## 3.1 Background

The method is based on the work of Cox, 1993 and McMeeking & Evans, 1990 and it can be expressed as:

$$\Delta K_{tip}(\Delta\bar{\sigma}) = \alpha^{\alpha/(\alpha-1)} K_{tip}^{max}(\bar{\sigma}_{max} = \alpha^{\alpha/(1-\alpha)}\Delta\bar{\sigma}) \qquad 5$$

where the crack tip cyclic range of stress intensity factor, $\Delta K_{tip}$, at an applied stress range, $\Delta\bar{\sigma}$, is scaled to a static problem with a crack tip stress intensity factor $K_{tip}^{max}$ at an applied stress $\bar{\sigma}_{max}$. The scaling of the fatigue problem to a static problem is achieved through the scaling factors $\alpha^{\alpha/(\alpha-1)}$ and $\alpha^{\alpha/(1-\alpha)}$.

In the following, we consider only the case of mode I cracking. For a crack growing under monotonic loading, the traction-separation (cohesive law) has the following form:

$$\sigma_n = \beta\, \delta_n^{\alpha}, \qquad \alpha > 0 \qquad 6$$

where $\beta$ is the "bridging stiffness" parameter. The parameter $\alpha$ can have different values depending on the failure mechanism e.g. 0.5 for sliding fibres of infinite strength, 1.0 for linear springs. In DACOMAT project, it is envisioned that $\alpha$ will be calculated from micromechanical modelling (D1.1). For cycling loading, the bridging tractions have the following form:

$$\left|\sigma_n - \sigma_{n_r}\right| = \alpha^{-\alpha}\beta\left|\delta_n - \delta_{n_r}\right|^{\alpha}, \quad \alpha > 0 \qquad 7$$

where $\sigma_{n_r}$ is the traction at the last load reversal and similarly $\delta_{n_r}$ is the opening at the last load reversal.

## 3.2 Cyclic cohesive laws

In order to investigate the applicability of the scaling approach, the finite element method was used as a tool to perform numerical experiments. For this reason, several cohesive laws were developed, and they are presented in this Section. All the cohesive laws were implemented as user-defined materials (UMAT) for Abaqus finite element software.

Figure 8 shows a cohesive law with a linear softening behaviour (static response) and the loading/unloading behaviour given in Eq. 7 for constant $\beta$ e.g. independent of the opening at which unloading occurs. As it can be seen unloading results in permanent opening opposed to the cohesive fatigue model of Section 2. In Figure 9, the traction-separation response from the finite element solution is compared to Eq. 7, for set of $\alpha$ and $\beta$ parameters, to validate the correct implementation

The DACOMAT project has received funding from the European Union's Horizon 2020 research and innovation programme under GA No. 761072

of the cohesive law in Abaqus. As it can be seen the finite element results are in excellent agreement with the analytical cohesive law for all the regimes including the unloading/reloading part.

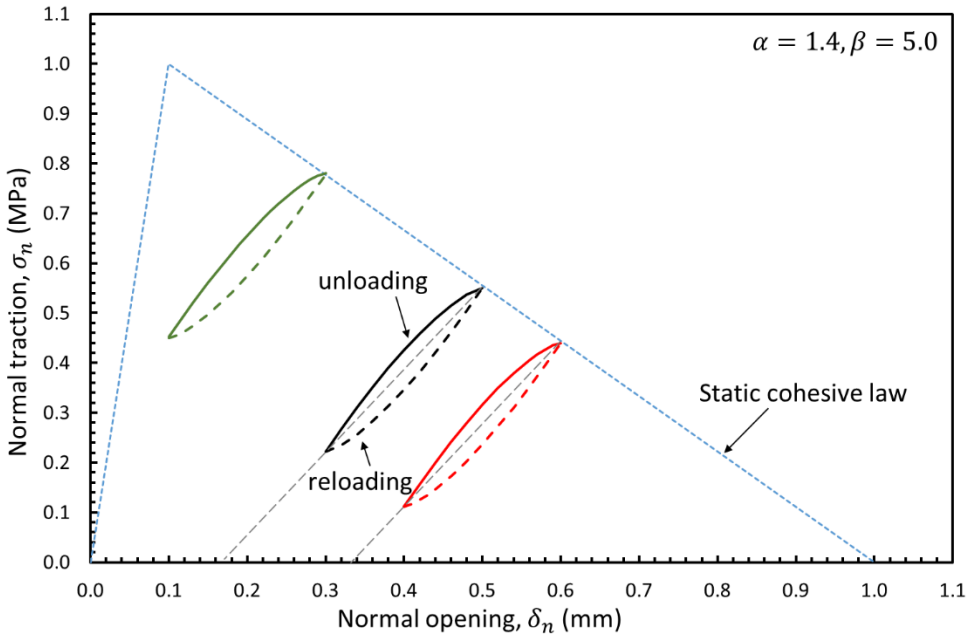


**Figure 8** Cohesive law with cyclic loading/unloading response in the linear softening regime with $\beta$ constant.

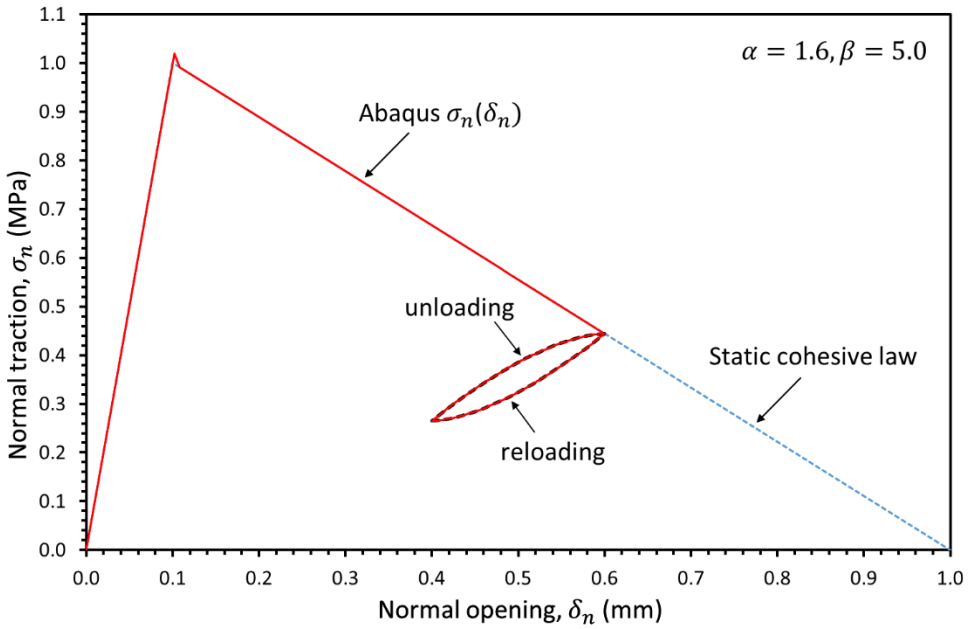


**Figure 9** Validation of the implement cohesive law of Eq. 7.

The cohesive law of Figure 8 requires that the crack tip is modelled as a singular field. This issue and the associated difficulties will be explained in more detail in the next section where the finite element will be described. An alternative approach is to use a cohesive law with bi-linear softening, as in D1.3, in order to separate the crack tip fracture process zone from the bridging zone. In this case, there is no

The DACOMAT project has received funding from the European Union's Horizon 2020 research and innovation programme under GA No. 761072

need to model the crack tip singularity. In Figure 10, the validation of the implemented cohesive law with-bilinear softening and Eq. 7 is shown. Figure 11 shows in more details the comparison between the finite element solution and Eq. 7 in the unloading and reloading regions. An excellent agreement of the numerical results with the analytical cohesive laws exists and thus the cohesive law is correctly implemented in Abaqus.

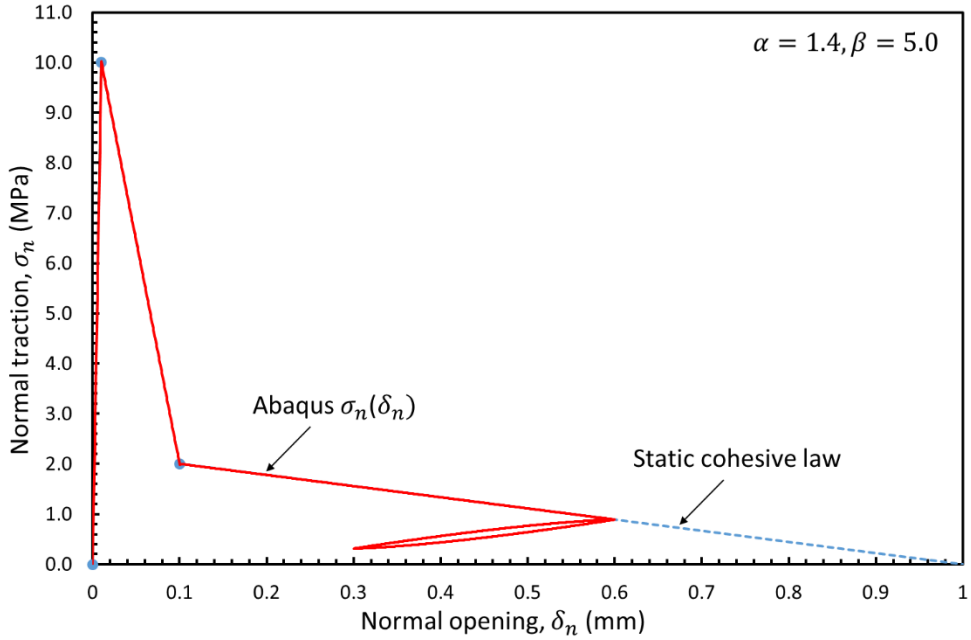


**Figure 10** Cohesive law with bi-linear softening to separate the crack tip fracture process zone from the bridging zone with $\beta$ constant. Validation of the Abaqus implemented cohesive law.

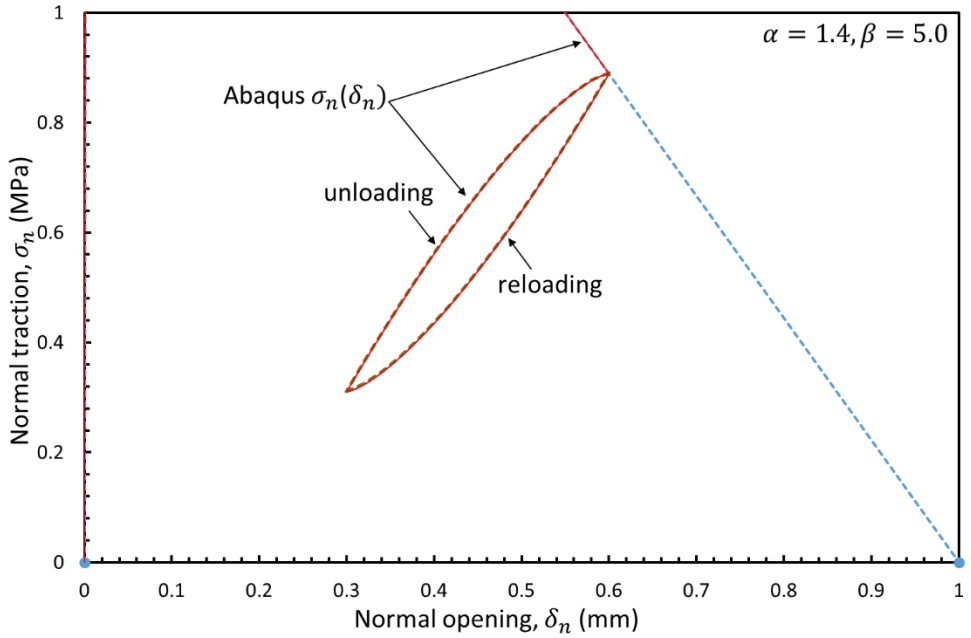


**Figure 11** Detailed view (from Figure 10) of the comparison between the finite element solution and Eq. 7 for the unloading and reloading response. $\beta$ is constant.

The DACOMAT project has received funding from the European Union's Horizon 2020 research and innovation programme under GA No. 761072

In the above cohesive laws, the cyclic loading (unloading/reloading) occurs in the softening part e.g. it is required that the static peak traction is reached prior to cyclic loading. As it mentioned in Section 2, this may not be realistic. Thus, a different cohesive law shown in Figure 12 is implemented in Abaqus. The response prior to the cyclic part is given by Eq. 6. As can be seen, the finite element solution agrees well with the analytical cohesive law.

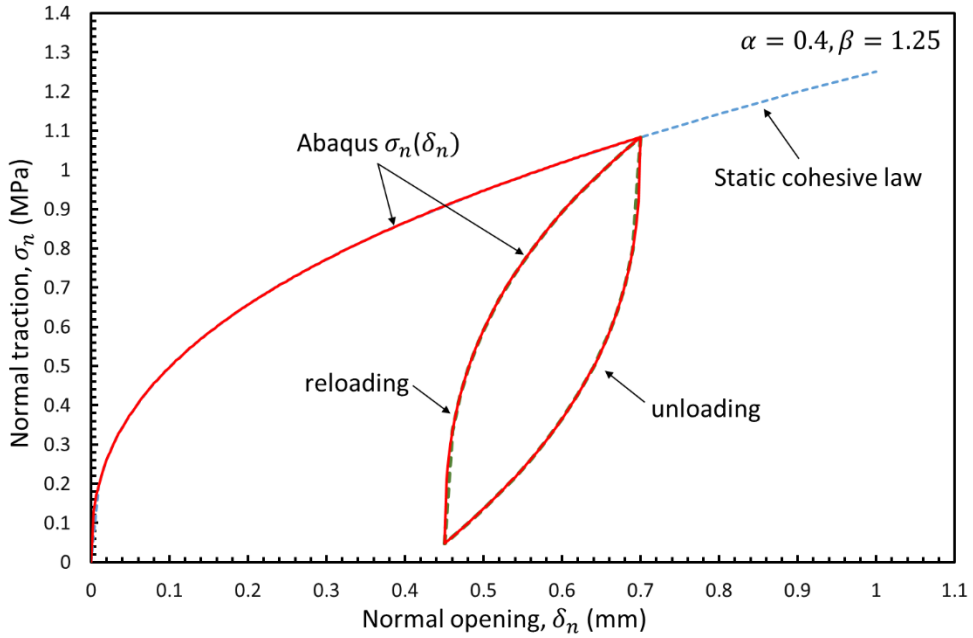


**Figure 12** A cohesive law whose response prior to cyclic loading is fully described by Eq. 6. The cyclic part is given by Eq. 7. $\beta$ constant *(McMeeking & Evans, 1990)*.

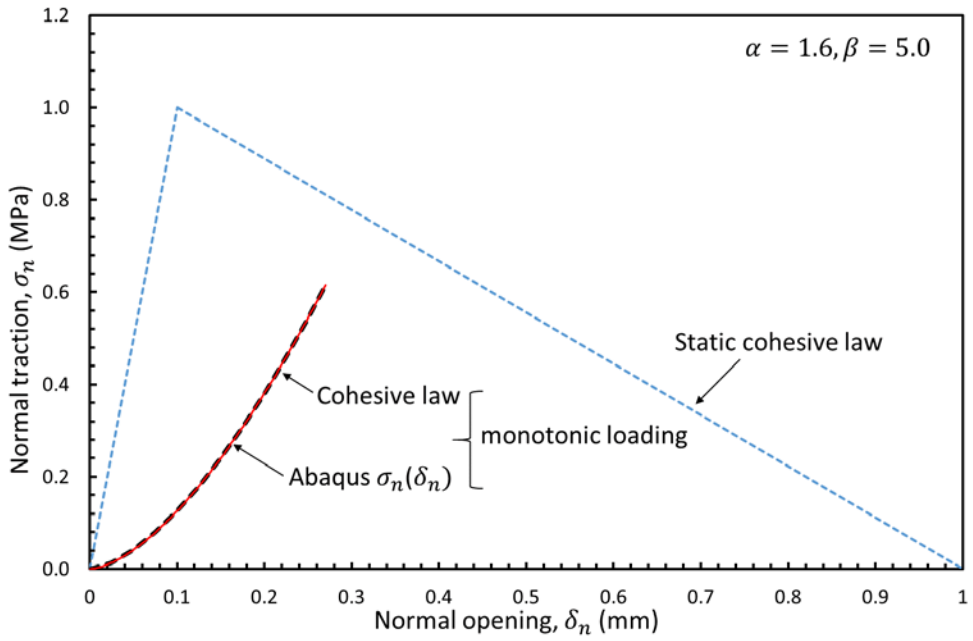


**Figure 13** Cohesive law for the monotonic loading solution required in Eq. 5.

The DACOMAT project has received funding from the European Union's Horizon 2020 research and innovation programme under GA No. 761072

Figure 13 shows the validation of the implemented cohesive law in Abaqus that is required for the equivalent static problem (see Eq. 5). This cohesive law is described by Eq. 6.

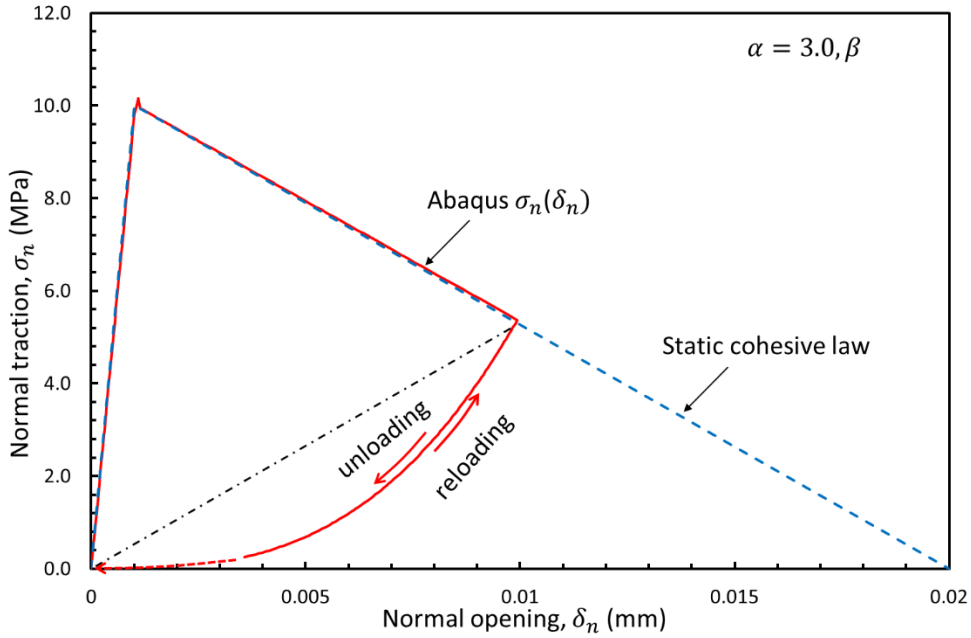


**Figure 14** Cohesive law with cyclic loading/unloading response in the linear softening regime with $\beta$ variable.

Figure 14 shows a different cohesive law. It is identical to the cohesive law of Figure 9 with the differences that β is not constant and the loading and reloading curves coincide. This cohesive law is inspired from the micromechanical mode of D1.1 where it was shown that the unloading and reloading curves are similar. It is also more natural that β depends on the opening when unloading occurs. In the current implementation, β is chosen in such way as to have zero permanent opening at complete unloading.

## 3.3 Model to test the scaling approach

Figure 15 shows the finite element model used to investigate the scaling approach. It is a DCB specimen (similar to the specimens used in WP3 to experimentally characterise the materials developed in DACOMAT). Simulations with both applied moments and applied forces were performed.

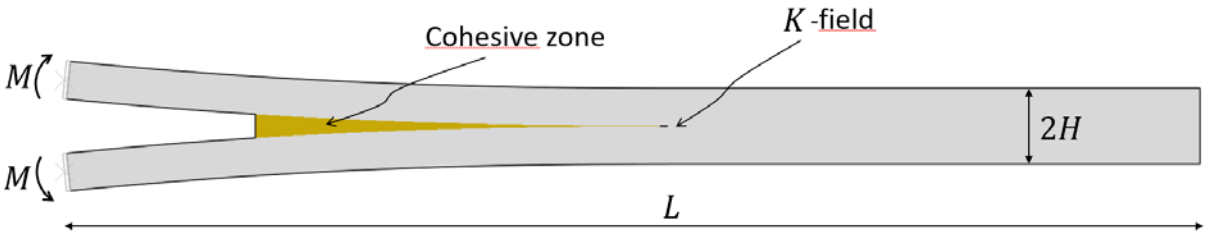


**Figure 15** Schematic illustration of the finite element model used to test the scaling approach. Both the K-field and the cohesive zone are modelled. A small gap exists between the two regions in order to compute $\Delta K_{tip}$ *and* $K_{tip}^{max}$.

The DACOMAT project has received funding from the European Union's Horizon 2020 research and innovation programme under GA No. 761072

The cohesive zone does not extend along the whole specimen length. Ahead (to the right) of the cohesive zone, there is a small gap and then there is the crack tip region. With this choice, $\Delta K_{tip}$ and $K_{tip}^{max}$ ahead of the bridging zone can be calculated using the J-integral. The existence of the gap is not ideal, and it creates uncertainties regarding the applied load required to have a realistic transition between the crack tip region and the cohesive zone. This issue is currently under investigation. It is for this reason, e.g. to avoid the gap, that the cohesive law of Figure 10 was implemented.

## 3.4 Initial results

Some initial results will be presented in this Section. It should be emphasised that these are preliminary results. It is planned to re-run the models and run more cases as well. Prior presenting the tables with the scaling results, a contour plot of the normal stresses is shown in Figure 16 for a cohesive similar to Figure 9.

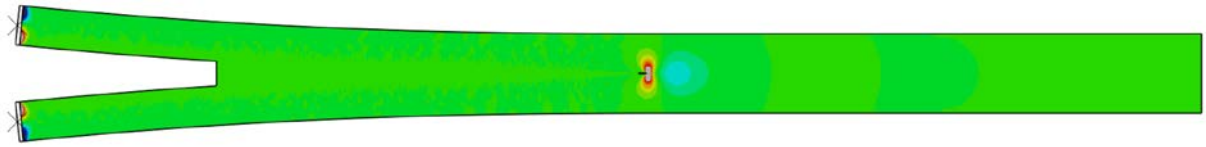

**Figure 16** Contour plot of the normal stresses showing the K-field at the crack tip.

Table 1 shows the scaling results when the cohesive law of Figure 9 was used. The DCB specimen was loaded with pure bending moments as shown in Figure 15. From the cyclic solution, $\Delta K_{tip}$ is calculated. Then two static simulations were run. In the first, the applied moment was scaled, and in the second the applied J. As it can be seen from Table 1, the scaling approach works when J is scaled. The same result was obtained when the DCB specimen was loaded with forces. However, according to the theory, the scaling approach should work by scaling the applied moments or forces and not the applied J.

**Table 1** Case 1 – cohesive law from Figure 9.

| **Cyclic loading** | | | | | | | | | |
|---|---|---|---|---|---|---|---|---|---|
| | $M$ N mm | $J_{ext}$ N/mm | $K_{tip}$ MPa $\sqrt{mm}$ | | $\Delta M$ N mm | $\Delta J_{ext}$ N/mm | $\Delta K_{tip}$ | | |
| Loading<br>Unloading<br>Reloading | 35.28<br>65.00 | 0.136<br>0.461 | 0.0073<br>0.0447 | | 29.72 | 0.3254 | 0.0374 | | |
| **Static loading – Moments scaling** | | | | | | | | | |
| $\alpha$ | $\alpha^{\alpha/(1-\alpha)}$ | $M$ | | | $J_{ext}$ | $K_{tip}$ | $\alpha^{\alpha/(\alpha-1)}$ | $K_{tip}^{max}$ | $\Delta K_{tip}/K_{tip}^{max}$ |
| 1.4 | 0.308 | 9.154 | | | 0.0091 | 0.0022 | 3.2467 | 0.0071 | **5.25** |
| **Static loading – Applied J scaling** | | | | | | | | | |
| $\alpha$ | $\alpha^{\alpha/(1-\alpha)}$ | $J$ | | | $J_{ext}$ | $K_{tip}$ | $\alpha^{\alpha/(\alpha-1)}$ | $K_{tip}^{max}$ | $\Delta K_{tip}/K_{tip}^{max}$ |
| 1.4 | 0.308 | 0.1002 | | | 0.1002 | 0.0117 | 3.2467 | 0.0381 | **0.98** |

The DACOMAT project has received funding from the European Union's Horizon 2020 research and innovation programme under GA No. 761072

Table 2 shows similar results as Table 1 but with the cohesive law of *Figure 12*. Again, it is found that the scaling works with the applied J and not as expected with the applied moments. The same results were obtained by applying forces instead of moments e.g. the scaling works when J is scaled.

**Table 2** Case 2 – cohesive law from Figure 12.

| **Cyclic loading** | | | | | | | | | |
|---|---|---|---|---|---|---|---|---|---|
| | $M$ N mm | $J_{ext}$ N/mm | $K_{tip}$ MPa $\sqrt{mm}$ | | $\Delta M$ N mm | $\Delta J_{ext}$ N/mm | $\Delta K_{tip}$ | | |
| Loading<br>Unloading<br>Reloading | 41.00<br>71.00 | 0.183<br>0.461 | 0.0555<br>0.0985 | | 30.0 | 0.3669 | 0.043 | | |
| **Static loading – Moments scaling** | | | | | | | | | |
| $\alpha$ | $\alpha^{\alpha/(1-\alpha)}$ | $M$ | | | $J_{ext}$ | $K_{tip}$ | $\alpha^{\alpha/(\alpha-1)}$ | $K_{tip}^{max}$ | $\Delta K_{tip}/K_{tip}^{max}$ |
| 0.75 | 0.4218 | 12.656 | | | 0.0175 | 0.0010 | 2.3704 | 0.0024 | **17.53** |
| **Static loading – Applied J scaling** | | | | | | | | | |
| $\alpha$ | $\alpha^{\alpha/(1-\alpha)}$ | $J$ | | | $J_{ext}$ | $K_{tip}$ | $\alpha^{\alpha/(\alpha-1)}$ | $K_{tip}^{max}$ | $\Delta K_{tip}/K_{tip}^{max}$ |
| 0.75 | 0.4218 | 0.1547 | | | 0.1547 | 0.0197 | 2.3704 | 0.0467 | **0.92** |

## 3.5 Future work

The results obtained so far are not as expected. It is found that the scaling works with the applied J and not the square root of J. Since this method (Approach B) will be more useful than Approach A in an industrial context, and since all the numerical tools necessary to investigate the approach are developed, we will continue studying the scaling approach.

The DACOMAT project has received funding from the European Union's Horizon 2020 research and innovation programme under GA No. 761072

## 4. Conclusions

It was planned to develop a tool to model fatigue crack growth. Two approaches were evaluated.

- The first approach, Approach A, is based on developing a cohesive element that can be used in a finite element program where the solution is obtained through many cycles. The approach is very general, but it is not computationally efficient. The task of implementing the cyclic cohesive element was completed.
- The second approach, Approach B, is much more computationally efficient since the cyclic problem is transformed to a static problem. Two simulations are enough. All the numerical tools to verify the method were developed. The initial results do not agree with the theory as the scaling works with the applied J (for a DCB specimen) and not the square root of J. It is recommended to continue to work on this method and possibly identify the source of this discrepancy.

The DACOMAT project has received funding from the European Union's Horizon 2020 research and innovation programme under GA No. 761072

## References

Bak, B. L., Sarrado, C., Turon, A., & Costa, J. (2014). Delamination under fatigue loads in composite laminates: A review on the observed. *Applied Mechanics Reviews, 66*, 060803.

Bak, B. L., Turon, A., Lindgaard, E., & Lund, E. (2017). A benchmark study of simulation methods for high-cycle fatigue-driven delamination based on cohesive zone models. *Composite Structures, 164*, 198–206.

Cox, B. N. (1993). Scaling for bridged cracks. *Mechanics of Materials, 15*, 87-98.

Davila, C. (2018). From S-N to Paris law with a new mixed-mode cohesive fatigue model. In A. Waas (Ed.), *American Society for Composites 2018*, (pp. 1-15). Seattle, Washington, USA.

McMeeking, R. M., & Evans, A. G. (1990). Matrix fatigue cracking in fiber composites. *Mechanics of Materials, 9*, 214-227.

Nguyen, O., Repetto, E. A., Ortiz, M., & Radovitzky, R. A. (2001). A cohesive model of fatigue crack growth. *International Journal of Fracture, 110*, 351-136.

Paris, P. C., Gomez, M. P., & Anderson, W. P. (1961). A rational analytic theory of fatigue. *Trend in Engineering, 13*, 9-14.

Roe, K. L., & Siegmund, T. (2003). An irreversible cohesive zone model for interface fatigue crack growth simulation. *ngineering Fracture, 70*, 209-232.

The DACOMAT project has received funding from the European Union's Horizon 2020 research and innovation programme under GA No. 761072